ANTIMICROBIAL AGENTS AND CHEMOTHERAPY, Sept. 2005, p. 3825–3832 Vol. 49, No. 9
0066-4804/05/$08.00+0 doi:10.1128/AAC.49.9.3825–3832.2005

Molecular Basis for Increased Susceptibility of Isolates with Atazanavir Resistance-Conferring Substitution I50L to Other Protease Inhibitors

Joseph Yanchunas, Jr.,[1] David R. Langley,[2] Li Tao,[1] Ronald E. Rose,[3] Jacques Friborg,[3] Richard J. Colonno,[3] and Michael L. Doyle[1]*

Departments of Gene Expression and Protein Biochemistry, Bristol-Myers Squibb Pharmaceutical Research Institute, Route 206 and Province Line Road, Princeton, New Jersey 08543-4000,[1] and Computer-Aided Drug Design[2] and Virology,[3] Bristol-Myers Squibb Pharmaceutical Research Institute, 5 Research Parkway, Wallingford, Connecticut 06492-7660

Received 17 February 2005/Returned for modification 19 April 2005/Accepted 16 June 2005

Protease inhibitors (PIs) are highly effective drugs against the human immunodeficiency virus (HIV), yet long-term therapeutic use is limited by emergence of HIV type 1 (HIV-1) protease substitutions that confer cross-resistance to multiple protease inhibitor drugs. Atazanavir is a highly potent HIV protease inhibitor with a distinct resistance profile that includes effectiveness against most HIV-1 isolates resistant to one or two PIs. The signature resistance substitution for atazanavir is I50L, and it is frequently (53%) accompanied by a compensatory A71V substitution that helps restore viability and increases atazanavir resistance levels. We measured the binding affinities of wild-type (WT) and I50L/A71V HIV-1 proteases to atazanavir and other currently approved PIs (ritonavir, lopinavir, saquinavir, nelfinavir, indinavir, and amprenavir) by isothermal titration calorimetry. Remarkably, we find that all of the PIs have 2- to 10-fold increased affinities for I50L/A71V protease, except for atazanavir. The results are also manifested by thermal stability measures of affinity for WT and I50L/A71V proteases. Additional biophysical and enzyme kinetics experiments show I50L/A71V protease is a stable enzyme with catalytic activity that is slightly reduced (34%) relative to the WT. Computational modeling reveals that the unique resistance phenotype of I50L/A71V protease likely originates from bulky tert-butyl groups at P2 and P2′ (specific to atazanavir) that sterically clash with methyl groups on residue L50. The results of this study provide a molecular understanding of the novel hypersusceptibility of atazanavir-resistant I50L/A71V-containing clinical isolates to other currently approved PIs.

Protease inhibitors (PIs) are an effective and widely used class of drugs against the human immunodeficiency virus (HIV). However, the long-term use of PIs is compromised by the emergence of drug-resistant variants that have amino acid residue substitutions in the target protein, HIV type 1 (HIV-1) protease (PR). Furthermore, some of the substitutions confer broad cross-resistance to multiple PIs. Presently correlations between genotypic changes and cross-resistance phenotype are poorly understood.

Atazanavir (ATV) is a potent azapeptide PI recently approved for the treatment of HIV-1 infection. It has excellent oral bioavailability and pharmacokinetics that allow once-daily dosing and exhibits a favorable lipid toxicity profile relative to other approved PIs. ATV also has a distinct cross-resistance profile relative to other currently approved PIs, with susceptibility maintained against 86% of ATV-naive isolates resistant to 1 to 2 PIs (6). Reduced susceptibility to ATV was also found to require several amino acid changes and was relatively modest in degree. The HIV-1 PR active-site substitution I50L has been identified as the ATV signature resistance substitution (5). The I50L substitution was found in 100% of clinical isolates from PI-naive patients who received ATV-containing regimens and exhibited virological failure in clinical trials. Half (53%) of the ATV-resistant I50L isolates also contained a commonly observed compensatory substitution, A71V. The A71 position is structurally remote from the PR active site, and it is known that the A71V substitution restores viability to I50L-containing viruses that are otherwise growth impaired (5). Biochemical studies have shown A71V enhances the enzymatic function of HIV-1 PR that has otherwise been enzymatically impaired by primary resistance substitutions (18).

Remarkably, the signature substitution I50L was found to correlate with increased susceptibilities to other currently approved PIs (5). Although the clinical significance of the increased susceptibility associated with the I50L substitution requires further clinical investigation, successful sequencing of PIs may preserve options for treatment with other PIs.

Using a series of biophysical experiments, we have investigated the clinically important I50L/A71V-substituted HIV-1 PR and its molecular interactions with ATV and several other currently approved PIs (Fig. 1). The results provide a molecular foundation for understanding the distinct resistance phenotype of the I50L substitution, including a quantitative determination of the binding affinities of the PIs for wild-type (WT) and I50L/A71V forms of PR. Understanding the molecular basis for the distinct PI cross-resistance profile of I50L/A71V will help with the development of improved PI-based treatment approaches.

MATERIALS AND METHODS

Reagents. ATV was synthesized at Bristol-Myers Squibb. All other drugs used in this study were purchased. The pharmacy-provided PI drugs were dissolved in water, extracted using nonpolar organic solvents, and subjected to a variety of chromatographic steps and crystallization to obtain PIs with a high degree of purity as determined by high-performance liquid chromatography-UV-mass

* Corresponding author. Mailing address: Gene Expression and Protein Biochemistry Department, Bristol-Myers Squibb Pharmaceutical Research Institute, Princeton, NJ 08543-4000. Phone: (609) 252-3175. Fax: (609) 252-6012. E-mail: michael.doyle@bms.com.

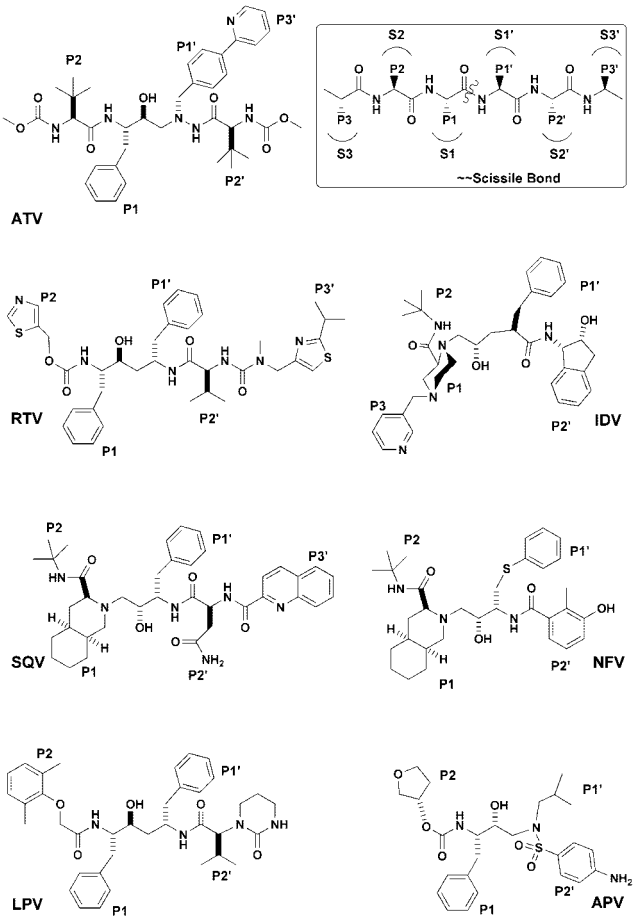

FIG. 1. Depiction of standard nomenclature (15, 22) used for the substrate residues (P1/P1′, etc.), their respective binding site pockets (S1/S1′, etc.), and corresponding group positions on inhibitors atazanavir (ATV), ritonavir (RTV), saquinavir (SQV), lopinavir (LPV), indinavir (IDV), nelfinavir (NFV), and amprenavir (APV).

spectrometry, nuclear magnetic resonance, and combustion analyses. An *Escherichia coli* codon-optimized PR gene from the HIV RF strain was PCR amplified from the pET-HIVPR expression vector (11), digested with BamHI and HindIII, and ligated into pET24d(+) (Novagen, Madison, WI). Amino acid substitutions Q7K, L33I, and L63I were introduced by site-directed mutagenesis into the PR to create a PR highly resistant to autolysis, pET24-TANG-RF-AUTO-C (17). The PR resistance substitutions I50L and A71V were introduced into pET24-TANG-RF-AUTO-C by site-directed mutagenesis as previously described (6), and sequences of the construct were verified by DNA sequence analysis.

Genes encoding wild-type (WT) and I50L/A71V recombinant HIV-1 PR in the expression vector pET24-TANG-RF-AUTO-C were transformed into *E. coli* BL21(DE3) host cells. Overexpression was induced with 1 mM isopropyl-β-D-thiogalactopyranoside in cultures at an optical density at 600 nm of 1.0 in Luria-Bertani broth at 37°C. Three hours after induction, the cells containing HIV PR in inclusion bodies were harvested by centrifugation, and pellets were stored at −80°C for purification. Frozen cells containing HIV PR were suspended in 20 mM Tris, 1 mM EDTA, 10 mM 2-mercaptoethanol, pH 7.5, and lysed in two cycles through a Niro Soavi Panda fluidizer at 4,800 kPa. The lysate was centrifuged at 20,000 × *g* for 20 min at 4°C, and the pellet containing the majority of the HIV PR was used for purification. Purification of HIV PR from the pellets, refolding, and final purification was done according to methods described elsewhere (19). The folded, purified PR was then loaded onto an SP Sepharose column to remove minor contaminants and eluted with 2 mM to 500 mM NaCl gradient. Fractions were pooled and concentrated to approximately 1 mg/ml for storage. Identities of the PR forms were confirmed by electrospray ionization mass spectrometry. Masses for WT and I50L/A71V PR were measured as 10,776 and 10,805 Da, respectively, and were within 1 Da of the values calculated from sequence.

Enzyme assay. HIV PR activity was measured by monitoring the hydrolysis of the chromogenic substrate, H-Lys-Ala-Arg-Val-Nle-p-nitro-Phe-Glu-Ala-Nle-NH_2 (Bachem Bioscience Inc., King of Prussia, PA), at 300 nm using a SpectraMax absorbance plate reader with path length correction, thermostated to 25°C. Reactions in 100 μl typically contained 25 to 100 nM PR and 1 to 100 μM substrate peptide in buffer containing 100 mM sodium acetate, pH 5.0, and 1.0 M NaCl. Protein concentrations for the two PR forms were determined by active-site titration with a common solution of ATV. Initial rates were determined from absorbance data using a molar extinction coefficient for the change in absorbance upon hydrolysis equal to 1,800 M^{-1} cm^{-1}. Data analysis was performed using Origin 7 software (Microcal Inc., Northampton, MA).

Isothermal titration calorimetry (ITC). Isothermal titration calorimetry experiments were carried out at 25°C in a VP-ITC microcalorimeter (Microcal Inc.). PR was dialyzed against 10 mM sodium acetate (pH 5.0) buffer. Sodium acetate has a very small proton ionization heat of −0.1 kcal/mol proton (8). Also, coupled protonation values have been measured for several PIs (indinavir [IDV], nelfinavir [NFV], saquinavir [SQV], and ritonavir [RTV]) under the conditions of this study and are known to be small with respect to the potential effect on the measured enthalpy change (0.1 to 0.6 protons released per PI bound) (27). The binding enthalpies we report are thus, within error (0.2 kcal/mol), equal to the true biochemical binding enthalpy changes. Protein concentrations were estimated after dialysis by absorbance using a molar extinction coefficient of 12,900 M^{-1} cm^{-1}. Inhibitor powders were dissolved in dimethyl sulfoxide (DMSO) just prior to use. All solutions for titration contained dialysis buffer with 2% (vol/vol) DMSO. In order to measure K_d values for the tight binding inhibitors, acetyl pepstatin (Bachem Bioscience Inc., King of Prussia, PA) was used as a competition displacement ligand (24, 29). Data were analyzed using the competition model in Origin 7 (Microcal) software. Acetyl pepstatin is especially attractive as a competition ligand for inhibitors that have little exothermic heat because its heat is endothermic. Thus, displacement of acetyl pepstatin generates an exothermic heat that is additive with the exothermic binding heat of the inhibitor. In a typical experiment, the calorimetry cell containing 20 μM PR dimer and 200 μM acetyl pepstatin was titrated with syringe solution containing 200 μM tight binding inhibitor.

Differential scanning calorimetry (DSC). DSC experiments on the WT and I50L/A71V recombinant HIV-1 PR were carried out similarly to the method described previously (28). Thermal unfolding of HIV-1 PR was monitored with a VP-DSC (Microcal Inc., Northampton, MA) at 1°C/min from 25 to 80°C in buffer containing 10 mM sodium formate, pH 3.4. Resulting scans were analyzed with Origin 7 (Microcal) software according to a two-species model that includes folded dimer and unfolded monomer.

Thermal stability enhancement studies. The thermal stability enhancement effects of inhibitors on WT and I50L/A71V HIV-1 PR was measured with a ThermoFluor instrument (3-Dimensional Pharmaceuticals, Inc., Yardley, PA) (3, 21). The technology measures thermal denaturation curves by monitoring the fluorescence enhancement of an extrinsic probe (1-anilino-8-naphthalene sulfonate [ANS], used in the present study) that binds preferentially to the unfolded protein. Reactions contained 0.2 mg/ml PR in the presence or absence of varying concentrations of PIs in final conditions of 10 mM sodium acetate, pH 5.0, 100 μM ANS, and 0.5% (vol/vol) DMSO. Reactions were monitored in 384-well plates (Abgene) by increasing temperature in 1°C increments with 60 s of equilibration at each temperature and measuring four 10-s exposure digital images (plus 1 dark field image) per point from 25 to 95°C. Thermal denaturation curves were analyzed with ThermoFluor Analysis software (3DP, Inc.) to determine T_m values (the temperature at which the unfolding reaction is half complete).

In theory the PI-induced increases in thermal stability can be used to calculate PI equilibrium binding constants. The calculations assume the binding and unfolding reactions are reversible and that the PIs bind specifically to the native state, not the denatured state. The theory and applications of the method have been described in detail previously (2, 21, 23, 26). The increase in thermal stability is related to the equilibrium dissociation constant (K_d) at T_m ($K_d^{T_m}$) according to the following equation:

$$K_d^{T_m} = \frac{[L]_{T_m}}{\left[\exp\left\{\frac{-\Delta H_U^{T_0}}{R}\left[\frac{1}{T_m}-\frac{1}{T_0}\right]+\frac{\Delta C_{pU}}{R}\left[\ln\left(\frac{T_m}{T_0}\right)+\frac{T_0}{T_m}-1\right]\right\}\right]-1}$$

where T_0 and T_m are the midpoint unfolding temperatures in the absence and presence of PI, respectively, $[L]_{Tm}$ is the unbound PI concentration at T_m, $\Delta H_U^{T_0}$ and ΔC_{pU} are the unfolding enthalpy and heat capacity changes in the absence

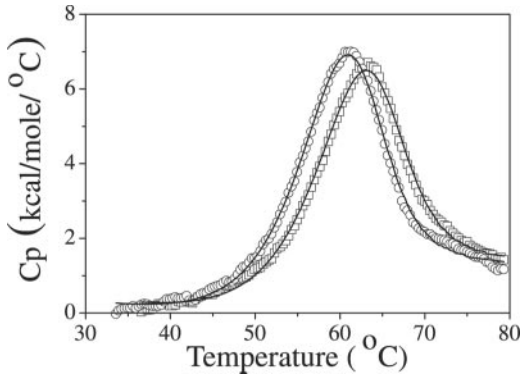

FIG. 2. Differential scanning calorimetry data for WT (circles) and I50L/A71V (squares) HIV-1 proteases. Conditions were 5 μM as dimer in 10 mM sodium formate and pH 3.4 where reversibility and unfolding models have been established (28). Data were fit (solid lines) to a model in which unfolding occurs concomitantly with dimer dissociation and no folded monomers are present.

of PI, and R is the gas constant (1.987 cal/degree mol). It is important to note that the $K_d^{T_m}$ values measured correspond to affinities at elevated temperature T_m. One may thus compare affinities at T_m directly from measured ΔT_m values.

It is also valuable to extrapolate the K_d values at T_m to a reference temperature, such as 25°C, where they can be compared to K_ds measured by another method. The temperature correction is done with the integrated van't Hoff equation (2, 7). The key physical quantity needed for the van't Hoff calculation is the PI binding enthalpy change, which was measured directly for all the PIs in this study by ITC. The binding enthalpy values are also dependent on temperature (7). To a very good approximation the enthalpy temperature dependence is linear and denoted as the binding heat capacity changes (ΔC_{pL}). Here we measured directly the ΔC_{pL} values of 0.470 ± 0.020 and −0.440 ± 0.040 kcal/mol degree for WT and I50L/A71V PR, respectively (data not shown). Values for ΔC_{pL} for APV, IDV, NFV, SQV, RTV, and acetyl pepstatin (−0.440, −0.450, −0.400, −0.340, −0.380, and −0.452 kcal/mol degree, respectively) were taken from literature reports corresponding to the same conditions as used in the present study (16, 20, 27). The ΔC_{pL} value for lopinavir (LPV) was not available, and due to difficulties in measuring it we used the average of literature values for 11 PIs (−0.414 ± 0.043 kcal/mol degree) as an approximation.

Structural modeling. The Protein Design module within QUANTA (Accelrys Corporation, San Diego, CA) was used to overlay the HIV PR/drug complexes and to insert the I50L substitution into the PR structure. The x-ray structures used in this study [capsid-p2, 1f7a (17a); IDV, 1hsg (4); LPV, 1mui (25); NFV, 1ohr (12); RTV, 1hxw (13); SQV, 1mtb (10); APV, 1hpv (22a)] were obtained from the Research Collaboratory for Structural Bioinformatics Protein Data Bank (PDB) (1) with the exception of the ATV structure (H. E. Klei, K. Kish, P.-F. Lin, Q. Guo, J. Friborg, R. E. Rose, Y. Zhang, V. Goldfarb, M. G. Wittekind, and S. Sheriff, unpublished data). The inhibitor structures were overlaid onto the capsid-p2 structure. The orientation with the lowest root mean squared deviation between Cα-carbons was used to define the P3 to P3′ directionality for each inhibitor, with the exception of 1mtb.pdb, which was fit so that SQV and NFV have the same P3 to P3′ orientation. The overlays were used to orient each inhibitor within the I50L/A71V form of PR. The I50L/A71V PR was generated by inserting substitutions into the x-ray structure of the ATV-PR complex. Graphics were generated using WebLab ViewerPro 4.0 (Accelrys).

RESULTS

Thermal stabilities of WT and I50L/A71V HIV-1 proteases. The thermal stabilities of WT and I50L/A71V HIV-1 PRs were examined by DSC. Figure 2 shows a comparison of the thermal stabilities of WT and I50L/A71V HIV-1 PR. The data were fit to a model that represents concomitant dissociation and unfolding of a dimer to an unfolded monomer, with the folded monomer species being unpopulated (28). Experiments were conducted in conditions where reversibility of the transition and suitability of the fitting model have been established (27, 28). The WT T_m and unfolding enthalpy change agree very well with results previously measured under the same conditions (28). Surprisingly, the I50L/A71V PR exhibited an increase in thermal stability of 2.2 degrees, from 61.0°C (WT) to 63.2°C (I50L/A71V). Best-fit enthalpy changes for WT and I50L/A71V PR were very similar (110.0 ± 0.4 and 107.0 ± 0.5 kcal/mol dimer, respectively), as were best-fit heat capacity changes (2.59 ± 0.07 and 2.65 ± 0.07 kcal/mol dimer/degree, respectively). Because HIV PR is a noncovalent dimer, its thermal stability is dependent on the concentration of PR. The curve-fitting model provides estimates of the T_m values extrapolated to PR reference concentration of 1 M dimer. The best-fit T_m values at 1 M dimer were estimated as 68.77 °C (±0.08°C) and 71.02 °C (±0.08°C) for the WT and I50L/A71V, respectively.

TABLE 1. Catalytic parameters for WT and I50L/A71V HIV-1 proteases[a]

HIV PR	k_{cat} (s^{-1})[b]	K_m (μM)[b]	k_{cat}/K_m (s^{-1} μM^{-1})
WT	4.6 ± 0.2	4.7 ± 0.8	0.96 ± 0.17
I50L/A71V	2.5 ± 0.1	4.0 ± 0.8	0.63 ± 0.13

[a] Conditions included 25 to 100 nM HIV-1 PR, 1 to 100 μM substrate, 100 mM sodium acetate, pH 5.0, 25°C, and 1.0 M NaCl.
[b] Standard deviations are from nonlinear least-squares analysis.

Catalytic activities of WT and I50L/A71V HIV-1 proteases. We also examined the enzyme activities of the two HIV-1 PR forms using the chromogenic substrate H-Lys-Ala-Arg-Val-Nle-p-nitro-Phe-Glu-Ala-Nle-NH_2. Table 1 summarizes the catalytic parameters for the two forms of the PR based on Michaelis-Menten analysis. The results for WT PR are in good agreement with previous studies, which reported values of $k_{cat} = 8.1 \pm 0.2\ s^{-1}$, $K_m = 14 \pm 1$ μM, and $k_{cat}/K_m = 0.58\ s^{-1}\ \mu M^{-1}$ using the same substrate but slightly different buffer conditions (19). The catalytic rate constant of I50L/A71V PR is about a factor of 2 slower than the WT, whereas its K_m value is more similar to that of the WT. The overall catalytic efficiency of k_{cat}/K_m of I50L/A71V is 66% of the WT. The combination of DSC and enzyme kinetics results indicates that the I50L/A71V double mutant is a well folded enzyme with slightly reduced catalytic activity.

Competition ITC. The binding affinities of the PIs examined were all too tight to measure directly by ITC (subnanomolar), except for acetyl pepstatin. We therefore conducted competition ITC experiments using acetyl pepstatin as the competition ligand, using procedures developed for HIV PR by Velazques-Campoy and colleagues (29). The competition ITC approach requires determination of the K_d and binding enthalpy change values for acetyl pepstatin binding to WT and I50L/A71V HIV-1 PRs. Table 2 lists these values for direct binding of the acetyl pepstatin to WT and I50L/A71V HIV-1 PRs. The binding affinity of I50L/A71V is slightly tighter than the WT.

Competition ITC data for ATV are shown in Fig. 3. Inspection of the ATV binding data for the WT (Fig. 3A) shows a steep transition curve, indicating that the affinity is extremely tight. In fact, the K_d value was too tight to reliably measure. We note that the time for approach to equilibrium at each incremental injection of ATV was longer than with the other PIs

TABLE 2. Thermodynamic parameters measured by ITC for inhibitor binding to HIV proteases[a]

PI	HIV PR	K_d in pM[a](SD)	ΔG in kcal/mol[c](SD)	ΔH (kcal/mol)[d]	$-T\Delta S$ (kcal/mol)[e]
Atazanavir	WT	≤10[f]	≤ −15.0	−4.6	≤ −10.4
Atazanavir	I50L/A71V	220 (± 13)	−13.16 (± 0.04)	−6.3	−6.9
Ritonavir	WT	100 (± 11)	−13.63 (± 0.07)	−2.5	−11.1
Ritonavir	I50L/A71V	≤10[f]	≤ −15.0	−8.0	≤ −7.0
Saquinavir	WT	280 (± 22)	−13.07 (± 0.05)	+2.0	−15.1
Saquinavir	I50L/A71V	100 (± 14)	−13.63 (± 0.09)	−1.5	−12.1
Lopinavir	WT	36 (± 7)	−14.24 (± 0.12)	+2.8	−17.0
Lopinavir	I50L/A71V	≤40[f]	≤ −14.17	+0.2	≤ −14.4
Indinavir	WT	590 (± 93)	−12.58 (± 0.10)	+2.1	−14.7
Indinavir	I50L/A71V	270 (± 33)	−13.04 (± 0.08)	−3.5	−9.5
Nelfinavir	WT	670 (± 110)	−12.51 (± 0.10)	+3.6	−16.1
Nelfinavir	I50L/A71V	160 (± 29)	−13.35 (± 0.12)	−1.2	−12.2
Amprenavir	WT	220 (± 27)	−13.16 (± 0.08)	−5.9	−7.3[b]
Amprenavir	I50L/A71V	180 (± 24)	−13.28 (± 0.09)	−9.5	−3.8
Acetyl pepstatin	WT	330,000 (± 25,000)	−8.84 (± 0.04)	+6.7	−15.5
Acetyl pepstatin	I50L/A71V	210,000 (± 38,000)	−9.10 (± 0.12)	+2.8	−11.9

[a] Conditions included 25°C, 10 mM sodium acetate, pH 5.0, and 2% (vol/vol) DMSO.
[b] K_d values for acetyl pepstatin are reported with standard deviations for the $n = 7$ (WT) or $n = 5$ (I50L/A71V) titrations. Standard errors on the remaining K_d values are from nonlinear least-squares analysis of individual competition ITC titrations.
[c] ΔG values were calculated from K_d values from $\Delta G = RT \ln(K_d)$, where R is the gas constant (1.987 cal/deg mol) and T is temperature.
[d] Errors for ΔH values are approximately ± 0.2 kcal/mol and were estimated from the standard deviations for WT ($n = 7$) and mutant acetyl pepstatin ($n = 5$) runs (±0.18 kcal/mol in both cases) together with the nonlinear least-squares errors for individual titrations (typically 0.07 kcal/mol).
[e] Errors for $-T\Delta S$ values are +0.23 kcal/mol or smaller and are dominated by the error in ΔH.
[f] Upper limit values are reported. Actual values are too tight to measure reliably with the method.

and required a longer time in between injections (10 min). Analysis of the data demonstrated the affinity of ATV binding to WT HIV PR is tighter than or equal to 10 pM. In contrast, the affinity of ATV for I50L/A71V PR is much weaker (K_d = 220 pM). The ATV affinity for I50L/A71V PR is therefore at least 22-fold weaker than the WT.

Table 2 lists the best-fit binding enthalpy changes and equilibrium dissociation constants for several PI drugs as measured

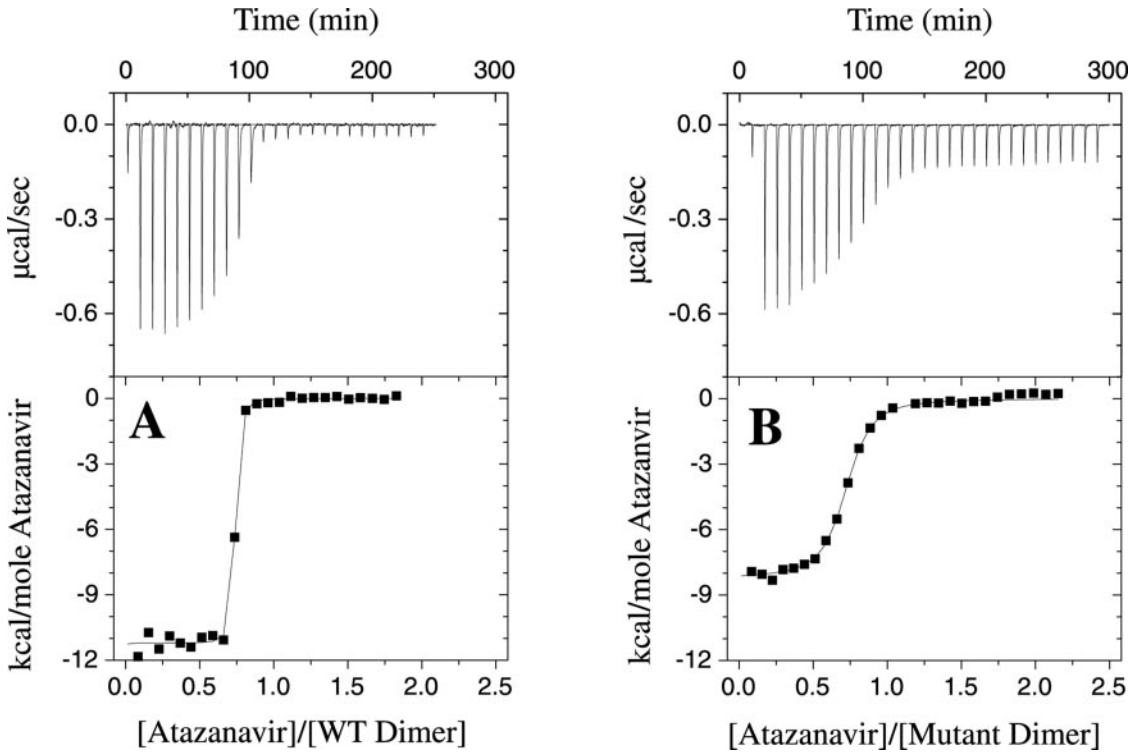

FIG. 3. Competition ITC data for titration of 200 μM ATV into HIV PR (20 μM as dimer in both cases). (A) WT; (B) I50L/A71V. The K_d for I50L/A71V was well resolved, whereas the value for WT was too tight to measure and only a K_d limit could be determined (Table 2). Conditions included 25°C, 10 mM sodium acetate, pH 5.0, 2% DMSO, and 200 μM acetyl pepstatin.

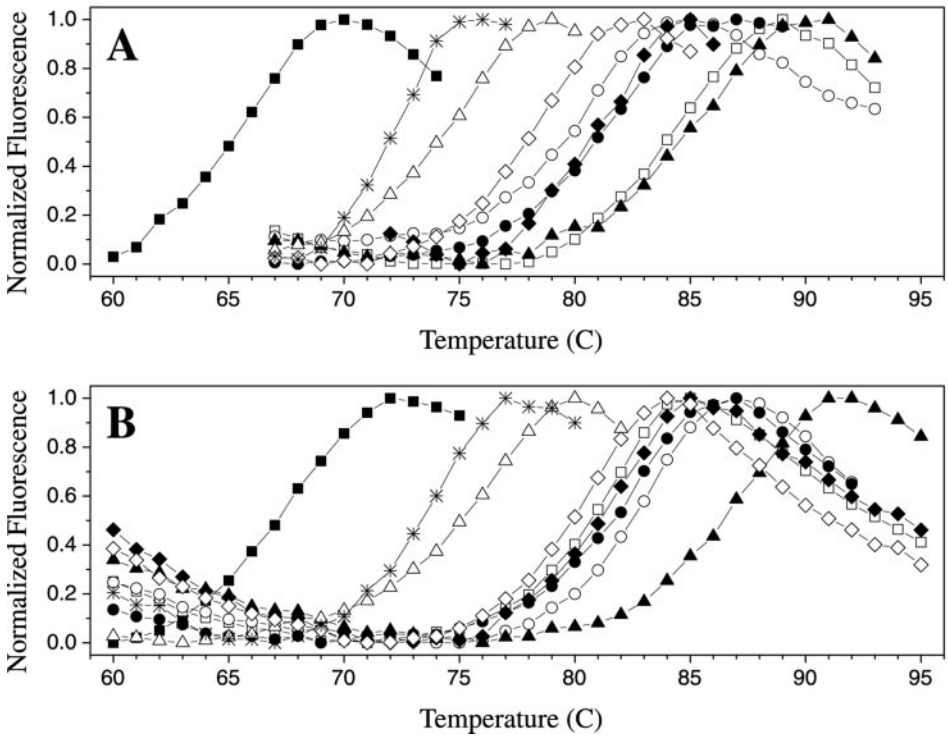

FIG. 4. Normalized ThermoFluor data for WT (A) and I50L/A71V (B) HIV-1 PR. Conditions included 10 mM sodium acetate, pH 5.0, 100 μM 1,8-ANS, 0.5% (vol/vol) DMSO, 3 μM protein, and 24 μM inhibitor. Inhibitors investigated were (■) control (no inhibitor); (□) ATV; (○) RTV; (●) SQV; (▲) LPV; (△) IDV; (◆) NFV; (◇) APV; and (*) acetyl pepstatin. Data at very low and high temperatures have been omitted from the figure for clarity and did not affect the calculated T_m values for those curves.

by competition ITC. All the K_d values were very well resolved, except the extremely tight binding cases of ATV binding the WT and RTV and LPV binding to I50L/A71V, wherein only upper-limit K_d values were determined. The PI binding ΔH and ΔG values for the WT are in excellent agreement with previous work conducted under the same conditions as the current study (19), except for ATV, for which results are not available for comparison. Interestingly, the I50L/A71V PR affinities of all inhibitors studied remained as tight as, or in some cases tighter than, the WT. The largest increase in binding affinity for I50L/A71V was seen for RTV, which binds the I50L/A71V mutant with an affinity that is at least 10-fold tighter than the WT.

Thermal stability enhancement. Although the affinities for most of the PIs binding to WT and I50L/A71V PR (Table 2) are rigorously characterized by ITC, the ITC measurements could only define upper limit K_d values for three interactions (ATV binding to WT as well as RTV and LPV binding to I50L/A71V). In order to investigate further the affinities of these interactions, we conducted thermal stability enhancement studies.

Thermal stability enhancement is especially useful for characterizing tight binding affinities. That is, the tighter the inhibitor, the greater the increase in thermal stability (2). Thermal unfolding curves for WT and I50L/A71V HIV-1 PRs in the presence and absence of PIs are shown in Fig. 4. The unfolding midpoint (T_m) for I50L/A71V PR in the absence of PI was found to be higher than the WT by about 2 degrees at pH 5.0. This was also observed by DSC at pH 3.4 (Fig. 2). Not surprisingly, the high-affinity PIs caused substantial increases in thermal stability of both PRs. The greatest stabilization was seen with LPV binding to I50L/A71V PR (ΔT_m = 21°C), while the smallest stabilization was seen with acetyl pepstatin binding to WT PR (ΔT_m = 6.4°C). ATV increased the T_m of WT PR by 4 degrees more than I50L/A71V PR, which is consistent with the considerably lower affinity of I50L/A71V PR demonstrated by ITC. Table 3 summarizes the thermal stability results as the increase in unfolding midpoint temperature (ΔT_m) for each PI. The ΔT_m values for LPV binding to WT and I50L/A71V PRs are very similar, with the I50L/A71V case showing a slightly

TABLE 3. Thermal stability enhancement (ΔT_m) of WT and I50L/A71V HIV-1 proteases by various PIs[a]

PR inhibitor	WT	I50L/A71V
Atazanavir	18.5	14.5
Ritonavir	14.5	16.5
Saquinavir	15.2	15.8
Lopinavir	20.4	21.0
Indinavir	9.5	9.8
Nelfinavir	15.5	15.0
Amprenavir	12.7	13.9
Acetyl pepstatin	6.4	6.6

[a] ΔT_m values (T_m with PI − T_m without PI) were determined by ThermoFluor from duplicate T_m values at 3 μM PR and 24 μM PI, together with the mean T_m values in the absence of PI for the WT (T_m = 66.7 ± 0.68°C, n = 13) and I50L/A71V (T_m = 67.9 ± 0.44°C, n = 14). Errors propagated for ΔT_m values are ± 0.95°C (WT) and ± 0.63°C (I50L/A71V).

TABLE 4. Relative PI binding parameters and vitality for WT versus I50L/A71V proteases at 25°C

PI	$\Delta\Delta H$[a] (kcal/mol)	ITC for K_d (I50L/A71V)/ K_d (WT)[b]	Thermal stability for K_d (I50L/A71V)/K_d (WT)[c]	Vitality[d]
Atazanavir	1.7	≥22	22 ± 10	≥14
Ritonavir	5.5	≤0.10	0.11 ± 0.04	≤0.07
Saquinavir	3.5	0.36 ± 0.06	0.46 ± 0.26	0.23 ± 0.07
Lopinavir	2.7	≤1.1	0.31 ± 0.10	≤0.73
Indinavir	5.6	0.46 ± 0.09	0.27	0.30 ± 0.10
Nelfinavir	4.8	0.24 ± 0.06	0.59 ± 0.20	0.16 ± 0.06
Amprenavir	3.6	0.82 ± 0.15	0.26 ± 0.12	0.54 ± 0.17
Acetyl pepstatin	3.9	0.64 ± 0.12	0.24 ± 0.06	0.42 ± 0.14

[a] $\Delta\Delta H = \Delta H$ (WT) − ΔH (I50L/A71V). Standard deviations are propagated from the values in Table 2 as ±0.28 kcal/mol.
[b] ITC K_d ratios and standard deviations are calculated from values in Table 2. Errors are indicated, except where only upper or lower limit values were determined.
[c] Thermal stability K_d ratios are the means from multiple K_d values calculated from multiple measurements of T_m at PI concentrations in the range of 6 to 96 mM. Means and standard deviations are from $n = 4$ determinations, except for Ritonavir with the WT ($n = 3$) and indinavir with the WT and lopinavir with I50L/A71V ($n = 2$, and the range was used as the error estimate). Indinavir with I50L/A71V is from a single determination, and an error was not calculated.
[d] Vitality = $(K_d k_{cat}/K_m)$ mutant/$(K_d k_{cat}/K_m)$WT using K_d values from ITC (9).

larger enhancement in stability. This indicates the LPV affinity is slightly greater for I50L/A71V at elevated temperature. Similar results are seen for RTV, although the enhanced stabilization of I50L/A71V is more pronounced. In general, all PIs except ATV are seen to stabilize I50L/A71V and WT PRs to a similar extent, indicating that their affinities at these elevated temperatures are similar for the two forms of the PR. NFV stabilizes WT slightly more than I50L/A71V at elevated temperature, suggesting it has a slightly higher affinity for WT near 80°C; however, after correcting the affinities to 25°C (see below and Table 4), the NFV affinity is slightly tighter to I50L/A71V.

As described in Materials and Methods, these ΔT_m values can be used to calculate PI binding affinities at 25°C so that they may be compared directly to the K_d values measured by ITC. Although K_d values calculated from the thermal stability method are not as rigorous as those measured by ITC, due to the multiple experimental parameters required for both the equation and the van't Hoff equation (2, 7), the analysis provides important qualitative insight into the magnitudes of the very high affinity interactions that cannot otherwise be resolved by ITC. Table 4 shows a comparison of relative affinities (ratio of K_ds for I50L/A71V and WT) determined by both ITC and thermal stability enhancement. We note that while the thermal unfolding curves measured at pH 5.0 were not reversible, the rank order of affinities correlates very well (Table 4) with those measured by ITC. This suggests that potential systematic error associated with irreversible unfolding does not contribute significantly to the data and its ability to be well described by the model represented by the equation. The thermal stability results indicate the ATV affinity of the mutant is reduced by an order of magnitude, whereas the RTV affinity is increased by an order of magnitude; both findings are in agreement with the ITC data. The thermal enhancement results also provide new insight into the extent to which LPV may bind mutants with higher affinity than the WT. The results in Table 4 indicate the LPV affinity for I50L/A71V is tighter than for the WT by a factor of 3. The remaining PIs exhibit two- to fourfold increased affinity for the mutant PR by the thermal stability method.

DISCUSSION

The hypersusceptibility phenotype of the atazanavir signature resistance substitution I50L to other currently approved protease inhibitors (5) is shown in the present study to correlate well with PI binding affinities that were determined with biophysical measurements. The results demonstrate that the affinities of several currently approved PIs are retained or increased toward the clinically important I50L/A71V-substituted PR. This is emphasized in Table 4, which lists the relative binding affinities of WT and I50L/A71V PRs as ratios of their K_d values. Table 4 also lists the changes in binding enthalpy ($\Delta\Delta H$ values) in going from WT to I50L/A71V substitutions. Interestingly, the binding enthalpies are more exothermic for all inhibitors binding to the I50L/A71V PR. However, the molecular basis for this observation is unclear.

We conducted structural modeling studies to understand the molecular features of I50L that lead to its unique resistance phenotype. Crystallographic studies (4, 10, 12, 13, 25, and H. E. Klei et al., unpublished) have shown that I50:A and I50:B (I50 residues in subunits A and B) sit between the S1/S2′ and S2/S1′ binding sites and interact with the P1/P2′ and P2/P1′ groups on the PR inhibitor, respectively. The t-butyl groups in ATV at P2 and P2′ (Fig. 1) form close van der Waal contacts with I50:B and I50:A in WT PR; however, an I50L substitution turns these favorable interactions into a minor steric hindrance for the t-butyl group at P2 and a major steric clash for the P2′ group (Fig. 5). The minor steric hindrance between ATV or SQV, IDV, and NFV (which have a single t-butyl group at P2 or P2′; Fig. 1) is readily relieved by a small conformational change in the PR flap containing L50:B. However, to relieve the major steric clash with the second t-butyl group that is unique to ATV, the A-domain flap must undergo a larger conformational change to make room for ATV. The slight opening of the active site to accommodate ATV results in a net gain in the binding enthalpy of 1.7 kcal/mol but is accompanied with a net loss in binding entropy of 3.5 kcal/mol, resulting in a net loss in the binding free energy of 1.8 kcal/mol (Tables 2 and 4). In the RTV and LPV complexes an I50L substitution packs up against the gem dimethyl group at P2′ and occupies the space taken up by the extra methyl group in the t-butyl group of ATV (Fig. 5). In SQV, IDV, NFV, and APV PI-PR complexes the L50 substitution packs against the planer aromatic (14) or amide group at P2′. In each case there is a substantial gain in the binding enthalpy (Tables 2 and 4) that more than compensates for the loss in the binding entropy. In contrast, most other

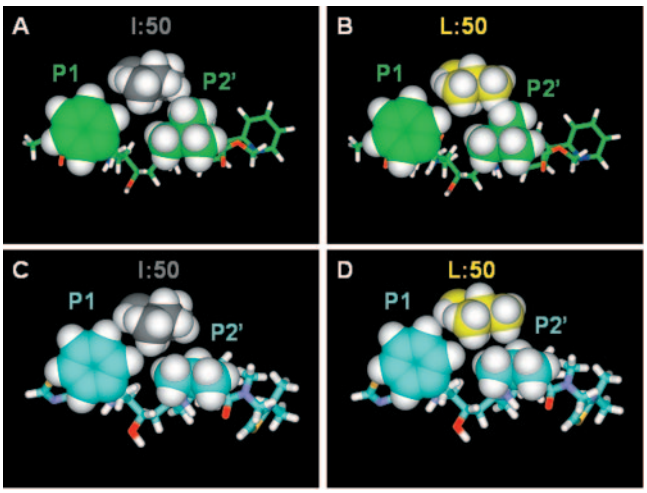

FIG. 5. (A and B) Atazanavir (carbon atoms are green) and (C and D) ritonavir (carbon atoms are turquoise) bound within WT (A and C; I50 carbons are gray) and I50L/A71V (B and D; L50 carbons are yellow) PR. Note that the favorable close van der Waal contact between I50 and an ATV tert-butyl group at P_2' (A) becomes an unfavorable steric clash (B) with the I50L substitution, while the weak distal van der Waal contact between I50 and an RTV gem dimethyl group at P_2' (C) becomes closer and more favorable with the I50L substitution (D). Noncarbon atom colors are the following: hydrogen, white; oxygen, red; nitrogen, blue; sulfur, dark yellow.

resistance mutations lead to a loss in enthalpic energy that is compensated by a gain in entropic energy (19, 30). The decrease in volume of the binding site for the I50L mutation and favorable interactions with most PIs may explain its unique thermodynamic profile.

The folding stability and catalytic properties of I50L/A71V PR were investigated to determine the extent that these properties might contribute to its resistance profile. It is known that the I50L substitution correlates with impaired viral growth and that the A71V substitution restores some viability (5), further increasing resistance to ATV. The DSC data in Fig. 2 indicate that the I50L/A71V PR has a high thermal stability, and in fact a thermal stability that is enhanced relative to the WT. Although it may be surprising that the mutant PR has increased thermal stability, similar results have been reported for the V82F/I84V active-site PI resistance substitution in HIV-1 PR (27). The enzymatic activity of I50L/A71V PR (Table 1) is modestly reduced relative to the WT PR (catalytic efficiency is 66% of WT) in the hydrolysis of the substrate H-Lys-Ala-Arg-Val-Nle-p-nitro-Phe-Glu-Ala-Nle-NH_2. Thus, the thermal stability and catalytic properties of I50L/A71V PR appear to be only slightly perturbed relative to WT PR.

Table 4 lists the biochemical vitality (9) of the I50L/A71V PR as predicted from the PI binding affinities and PR catalytic parameters measured in this study. The biochemical vitality parameter represents the relative PR activity of I50L/A71V PR versus WT PR under the inhibitory pressure of each inhibitor. Since the catalytic efficiency of I50L/A71V is close to (66% of) the WT, the trends in biochemical viabilities in Table 4 are largely governed by relative PI affinities. As expected from the greatly reduced ATV affinity of I50L/A71V PR, the viral vitality of I50L/A71V PR is predicted to be enhanced by an order of magnitude relative to WT. In contrast, all of the other PIs display an enhanced biochemical susceptibility to the I50L/A71V PR.

The present findings provide a molecular foundation for understanding the novel PI susceptibilities of clinical isolates containing the I50L substitution (5). The relative levels of PI affinities observed in the current study closely mimic the relative ATV resistance and increased susceptibilities to other PIs obtained using recombinant I50L/A71V viruses and proteases in cell culture assays (S. Weinheimer, L. Discotto, J. Friborg, H. Yang, and R. Colonno, unpublished data) and in human studies (5). Interestingly, the I50L substitution also counteracted the effect of several well-characterized PI resistance mutations when combined in similar PR backgrounds and further increased susceptibilities to PIs. The present results provide a molecular foundation for understanding the novel PI susceptibility profile inherent to I50L-containing viruses observed in vitro. The clinical relevance of the I50L resistance profile and the potential to preserve future treatment options will need to await further clinical data.

ACKNOWLEDGMENT

We thank Dianlin Xie for assistance with subcloning.

REFERENCES

1. **Berman, H. M., J. Westbrook, Z. Feng, G. Gilliland, T. N. Bhat, H. Weissig, I. N. Shindyalov, and P. E. Bourne.** 2000. The Protein Data Bank. Nucleic Acids Res. **28:**235–242.
2. **Brandts, J. F., and L. N. Lin.** 1990. Study of strong to ultratight protein interactions using differential scanning calorimetry. Biochemistry **29:**6927–6940.
3. **Carver, T. E., B. Bordeau, M. D. Cummings, E. C. Petrella, M. J. Pucci, L. E. Zawadzke, B. A. Dougherty, J. A. Tredup, J. W. Bryson, J. Yanchunas, Jr., M. L. Doyle, M. R. Witmer, M. I. Nelen, R. L. DesJarlais, E. P. Jaeger, H. Devine, E. D. Asel, B. A. Springer, R. Bone, F. R. Salemme, and M. J. Todd.** 2005. Decrypting the biochemical function of an essential gene from Streptococcus pneumoniae using ThermoFluor(R) technology. J. Biol. Chem. **280:**11704–11712.
4. **Chen, Z., Y. Li, E. Chen, D. Hall, P. Darke, C. Culberson, J. Shafer, and L. Kuo.** 1994. Crystal structure at 1.9-A resolution of human immunodeficiency virus (HIV) II protease complexed with L-735,524, an orally bioavailable inhibitor of the HIV proteases. J. Biol. Chem. **269:**26344–26348.
5. **Colonno, R., R. Rose, C. McLaren, A. Thiry, N. Parkin, and J. Friborg.** 2004. Identification of I50L as the signature atazanavir (ATV)-resistance mutation in treatment-naive HIV-1-infected patients receiving ATV-containing regimens. J. Infect. Dis. **189:**1802–1810.
6. **Colonno, R. J., A. Thiry, K. Limoli, and N. Parkin.** 2003. Activities of atazanavir (BMS-232632) against a large panel of human immunodeficiency virus type 1 clinical isolates resistant to one or more approved protease inhibitors. Antimicrob. Agents Chemother. **47:**1324–1333.
7. **Doyle, M. L., and P. Hensley.** 1997. Methods in enzymology, vol. 295. Academic Press, San Diego, Calif.
8. **Goldberg, R. N., N. Kishore, and R. M. Lennen.** 2002. Thermodynamic quantities for the ionization reactions of buffers. J. Phys. Chem. Ref. Data **31:**231–370.
9. **Gulnik, S. V., L. I. Suvorov, B. Liu, B. Yu, B. Anderson, H. Mitsuya, and J. W. Erickson.** 1995. Kinetic characterization and cross-resistance patterns of HIV-1 protease mutants selected under drug pressure. Biochemistry **34:**9282–9287.
10. **Hong, L., X. Zhang, J. Hartsuck, and J. Tang.** 2000. Crystal structure of an in vivo HIV-1 protease mutant in complex with saquinavir: insights into the mechanisms of drug resistance. Protein Sci. **9:**1898–1904.
11. **Ido, E., H.-P. Han, F. J. Kezdy, and J. Tang.** 1991. Kinetic studies of human immunodeficiency virus type 1 protease and its active-site hydrogen bond mutant A28S. J. Biol. Chem. **266:**24359–24366.
12. **Kaldor, S. W., V. J. Kalish, I. Davies, F. Jay, B. V. Shetty, J. E. Fritz, K. Appelt, J. A. Burgess, K. M. Campanale, N. Y. Chirgadze, D. K. Clawson, B. A. Dressman, S. D. Hatch, D. A. Khalil, M. B. Kosa, P. P. Lubbehusen, M. A. Muesing, A. K. Patick, S. H. Reich, K. S. Su, and J. H. Tatlock.** 1997. Viracept (nelfinavir mesylate, AG1343): a potent, orally bioavailable inhibitor of HIV-1 protease. J. Med. Chem. **40:**3979–3985.
13. **Kempf, D., K. Marsh, J. Denissen, E. McDonald, S. Vasavanonda, C. Flentge, B. Green, L. Fino, C. Park, X. Kong, N. Wideburg, A. Saldivar, L.**

Ruiz, W. Kati, H. Sham, T. Robins, K. Stewart, A. Hsu, J. Plattner, J. Leonard, and D. Norbeck. 1995. ABT-538 is a potent inhibitor of human immunodeficiency virus protease and has high oral bioavailability in humans. Proc. Natl. Acad. Sci. USA **92:**2484–2488.

14. **Kim, E., S. Paliwal, and C. S. Wilcox.** 1998. Measurements of molecular electrostatic field effects in edge to-face aromatic interactions and CH-π interactions for protein folding and molecular recognition. J. Am. Chem. Soc. **120:**11192–11193.
15. **Leung, D., G. Abbenante, and D. P. Faielie.** 2000. Inhibitors: current status and future prospects. J. Med. Chem. **43:**305–341.
16. **Luque, I., M. J. Todd, J. Gomez, N. Semo, and E. Freire.** 1998. Molecular basis of resistance to HIV-1 protease inhibition: a plausible hypothesis. Biochemistry **37:**5791–5797.
17. **Mildner, A. M., D. J. Rothrock, J. W. Leone, C. A. Bannow, J. M. Lull, I. M. Reardon, J. L. Sarcich, W. J. Howe, C.-s. C. Tomich, C. W. Smith, R. L. Heinrikson, and A. G. Tomasselli.** 1994. The HIV-1 protease as enzyme and substrate: mutagenesis of autolysis sites and generation of a stable mutant with retained kinetic properties. Biochemistry **33:**9405–9413.
18. **Nijhuis, M., R. Schuurman, D. de Jong, J. Erickson, E. Gustchina, J. Albert, P. Schipper, S. Gulnik, and C. Boucher.** 1999. Increased fitness of drug resistant HIV-1 protease as a result of acquisition of compensatory mutations during suboptimal therapy. AIDS **13:**2349–2359.
19. **Ohtaka, H., A. Schon, and E. Freire.** 2003. Multidrug resistance to HIV-1 protease inhibition requires cooperative coupling between distal mutations. Biochemistry **42:**13659–13666.
20. **Ohtaka, H., A. Velazques-Campoy, D. Xie, and E. Freire.** 2002. Overcoming drug resistance in HIV-1 chemotherapy: the binding thermodynamics of amprenavir and TMC-126 to wild-type and drug-resistant mutants of the HIV-1 protease. Protein Sci. **11:**1908–1916.
21. **Pantoliano, M. W., E. C. Petrella, J. D. Kwanoski, V. S. Lovanov, J. Myslik, E. Graf, T. Carver, E. Asel, B. A. Springer, P. Lane, and F. R. Salemme.** 2001. High-density miniaturized thermal shift assays as a general strategy for drug discovery. J. Biomol. Screening **6:**429–440.
22. **Schechter, I., and A. Berger.** 1967. On the size of the active site in protease. I. Papain. Biochem. Biophys. Res. Commun. **27:**157–162.
23. **Schellman, J. A.** 1975. Macromolecular binding. Biopolymers **14:**999–1018.
24. **Sigurskjold, B. W.** 2000. Exact analysis of competition ligand binding by displacement isothermal titration calorimetry. Anal. Biochem. **277:**260–266.
25. **Stoll, V., W. Qin, K. D. Stewart, C. Jakob, C. Park, K. Walter, R. L. Simmer, R. Helfrich, D. Bussiere, and J. Kao.** 2002. X-ray crystallographic structure of ABT-378 (Lopinavir) bound to HIV-1 protease. Bioorg. Med. Chem. **10:**2803–2806.
26. **Straume, M., and E. Freire.** 1992. Two-dimensional differential scanning calorimetry simultaneous resolution of intrinsic protein structural energetics and ligand binding interactions by global linkage analysis. Anal. Biochem. **203:**259–268.
27. **Todd, M. J., I. Luque, A. Velazques-Campoy, and E. Freire.** 2000. Thermodynamic basis of resistance to HIV-1 protease inhibition: calorimetric analysis of the V82F/I84V active site mutant. Biochemistry **39:**11876–11883.
28. **Todd, M. J., N. Semo, and E. Freire.** 1998. The structural stability of the HIV-1 protease. J. Mol. Biol. **283:**475–488.
29. **Velazques-Campoy, A., Y. Kiso, and E. Freire.** 2001. The binding energetics of first- and second-generation HIV-1 protease inhibitors: implications for drug design. Arch. Biochem. Biophys. **390:**169–175.
30. **Velazques-Campoy, A., S. Vega, and E. Freire.** 2002. Amplification of the effects of drug resistance mutations by background polymorphisms in HIV-1 protease from African subtypes. Biochemistry **41:**8613–8619.